Supporting Information

Bottom-Up Wet-Chemical Synthesis of a Two-Dimensional Porous Carbon Material with High Supercapacitance using a Cascade Coupling/Cyclization Route

Yongjie Xu,[a,b,c] *Reiner Sebastian Sprick,*[b] *Nick J. Brownbill,*[b,d] *Frédéric Blanc,*[b,d] *Qingyin Li,*[a] *John W. Ward,*[b,c]* *Shijie Ren,*[a]* *Andrew I. Cooper*[b,c]*

[a] College of Polymer Science and Engineering, State Key Laboratory of Polymer Materials Engineering, Sichuan University, Chengdu 610065, P. R. China.

[b] Department of Chemistry and Materials Innovation Factory, University of Liverpool, Liverpool L69 7ZD, UK.

[c] Leverhulme Research Centre for Functional Materials Design, University of Liverpool, Liverpool, UK.

[d] Stephenson Institute for Renewable Energy, University of Liverpool, Liverpool L69 7ZD UK.

Prof. A. I. Cooper. E-mail: aicooper@liverpool.ac.uk; Prof. S. Ren. E-mail: rensj@scu.edu.cn; Dr J. W. Ward. E-mail: john.ward@liverpool.ac.uk

Experimental details

Chemicals. Carbon tetrabromide and trimethylsilylacetylene were obtained from Sigma-Aldrich. *n*-Butyllithium, triphenylphosphine, pyridinium chlorochromate (PCC), methyl formate, anhydrous *N*, *N*–dimethylformamide (DMF) and triethylamine were obtained from Adamas Reagent, Ltd (China). Reduced graphene oxide (rGO) was obtained from the Sixth Elementary Materials Technology Co., Ltd (Changzhou, China). All reagents were used without further purification. Tetrahydrofuran (THF) was dried over sodium benzophenone and distilled, CH_2Cl_2 was dried over CaH_2 and distilled. Compounds **1**, **2**, **3** were synthesized using previously reported procedures.[1]

General methods. Air sensitive reactions were performed under argon using standard Schlenk techniques. Glassware was oven-dried overnight or dried using a heat gun.

Material characterization. Fourier transform infrared (FT-IR) spectroscopy studies were conducted on a Nicolet 560 Fourier-transform IR-spectrometer. Raman spectra were recorded on a LabRAM HR Raman Microscope with an excitation length of 633 nm. The nanomorphology of the bulk product was characterized by transmission electron microscopy (TEM, FEI Tecnai G2 F20 S-TWIN). Scanning electron microscope (SEM) studies were carried out at a JEOL JSM-5900LV microscope with a field emission cathode. Powder X-ray diffraction (PXRD) patterns were measured with a Philips X'Pert PRO MPD. Thermogravimetric analyses (TGA) were performed on a Netzsch 209 TG Stare System under N_2 flow. X-ray photoelectron spectroscopy (XPS) was carried out on a Kratos ASAM 800, performing at 12 kV and 15 mA with a monochromatic Al Kα source (hν = 1486.6 eV). The nitrogen and carbon dioxide adsorption-desorption measurements were performed on a BELSORB Max (BEL Japan Inc.). The surface areas were calculated from the adsorption branch of the isotherm by using the BET model in the pressure range P/P_0 from 0.05–0.3. The total pore volume was determined at a relative pressure of 0.99. The pore size distribution was analyzed from the gas adsorption data using a NLDFT method with a slit pore model. The liquid-state NMR spectra were collected on a Bruker ASCEND 400 spectrometer operating at 400 MHz in deuterated chloroform solution with TMS as reference. All solid-state NMR experiments were performed on a 400 MHz 9.4 T Bruker Avance III HD solid-state NMR spectrometer equipped with a 4 mm HXY triple-resonance magic angle spinning (MAS) probe (in double resonance mode) with the ^1H channel tuned to ^1H at $\nu_0(^1H) = 400.13$ MHz and the X

channel tuned to ^{13}C at $\nu_0(^{13}C)$ = 100.62 MHz. Experiments were performed at room temperature under MAS at ν_r = 10 kHz. ^{1}H, ^{13}C pulses and SPINAL-64 heteronuclear decoupling[2] during all ^{13}C detection were performed at a radiofrequency (rf) field amplitude of 83 kHz. The directly excited ^{13}C spectra in Figures 1b and S3 were performed with arbitrary recycle delays of 60 s and 0.5 h, and with 320 and 128 scans, respectively. The ^{1}H ^{13}C polarisation transfer in the cross polarization (CP) MAS experiments were obtained with a ^{13}C rf field of 60 kHz, while the ^{1}H rf field amplitude was ramped to obtain maximum signal at a ^{1}H rf field of approximately 60 kHz. CP MAS spectra were obtained with a recycle delay of 3 s (corresponding to 1.3 × $T_1(^{1}H)$ with $T_1(^{1}H)$ the spin lattice relaxation time measured using a saturation recovery sequence) and with contact times of 2 ms (and 256 scans) and 50 μs (and 64 scans). The ^{13}C chemical shifts were referenced to the CH carbon of adamantane at 29.45 ppm.[3] Samples were packed in a zirconia rotor with a KelF cap, and NMR data were obtained and analyzed using TopSpin 3.2.

Electrochemical measurements. The electrochemical experiments were carried out using a conventional, aqueous three-electrode system employing 6 M aqueous KOH as electrolyte at ambient temperature. The three-electrode cell incorporates SCE (saturated calomel electrode) as reference electrode, Pt as counter electrode. After removing oxygen containing groups through a heat-treatment, 2D-PCM was used as working electrode. The working electrode was prepared by grinding active materials (2D-PCM, 70 wt.%), conductive additive (acetylene black, 20 wt.%), and binder (polyvinylidene fluoride, 10 wt.%) in a mortar. The Ni foam current collector was coated with the slurry, dried under vacuum at 120 °C for 12 hours and then cut to a circle shape working electrodes with diameter of 12 mm. The following cyclic voltammetry (CV), galvanostatic charge/discharge (GCD) measurements and electrochemical impedance spectroscopy (EIS) were performed using a CHI 660E electrochemical workstation.

Calculation of specific power (P) and specific energy (E). The specific capacitance C (F g^{-1}), specific energy density E (Wh kg^{-1}) and specific power density P (W kg^{-1}) were calculated by the following equations, respectively: $C = I\Delta t/m\Delta V$, $E = 0.5C(\Delta V)^2/3.6$, $P = E/(\Delta t/3600)$, where C (F g^{-1}) is the experimentally determined specific capacitance, I (mA) is the discharge current, and Δt (s), m (mg), and ΔV (V) are the total discharge time, the mass of active material, and the potential drop (by excluding the voltage (IR) drop) during discharge, respectively.

Scheme S1. Synthesis of **1**.

Synthesis of 1,5-bis(trimethylsilyl)-1,4-pentadiyn-3-ol (S1).[1]

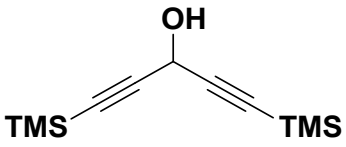

n-Butyllithium (39.6 mL, 63.4 mmol, 1.6 M in hexanes) was slowly added to a solution of trimethylsilylacetylene (9 mL, 63.4 mmol) in THF (60 mL) at -78 °C over the course of 30 minutes. After stirring the colorless mixture was 15 minutes, methyl formate (1.96 mL, 31.6 mmol) was added dropwise at 0 °C and the bright yellow mixture was heated to near reflux using a heat gun. Once cooled to room temperature, the mixture was poured into a beaker containing ethyl acetate (150 mL) and NH_4Cl solution (150 mL, saturated aqueous) and stirred for 5 minutes. Then the mixture was extracted with ethyl acetate and the combined organic layers were washed with water (150 mL) and brine (150 mL). The organic phases were dried with Na_2SO_4, filtered and concentrated to give a black oil. The oil was purified by flash chromatography ($CHCl_2$, silica) giving 1,5-bis(trimethylsilyl)-1,4-pentadiyn-3-ol (**S1**) as a yellow oil in 90% yield (6.4 g). ^{1}H NMR δ [ppm]: 5.09 (d, J = 7.0 Hz, 1 H), 2.24 (d, J =7.0 Hz, 1 H) 0.19 (s, 18 H). ^{13}C{^{1}H} NMR δ [ppm]: 101.6, 89.7, 53.0, -0.4.

Synthesis of 1,5-bis(trimethylsilyl)-1,4-pentadiyn-3-one (S2).[1]

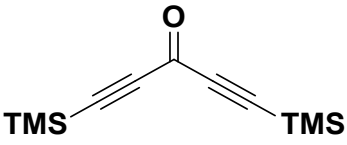

Pyridinium chlorochromate (9.31g, 43.2 mmol) was added to a solution of 1,5-bis(trimethylsilyl)-1,4-pentadiyn-3-ol (**1**) (6.45g, 28.8 mmol) in CH_2Cl_2 (anhydrous, 150 mL). The mixture was stirred for 2 hours at room temperature and filtered with DCM through a short plug of silica gel. The filtrate was dried over Na_2SO_4, filtered and concentrated giving 1,5-bis(trimethylsilyl)-1,4-pentadiyn-3-one (**S2**) as colorless needles in 90% yield (5.76 g). ^{1}H NMR δ [ppm]: 0.26 (s, 18 H). ^{13}C{^{1}H} NMR δ [ppm] 160.52, 102.66, 99.66, -0.73.

Synthesis of 3-(dibromomethylidene)-1,5-bis(trimethylsilyl)penta-1,4-diyne (1).[1]

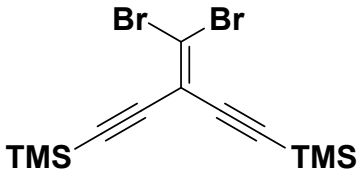

Triphenylphosphine (13.36 g, 51.0 mmol) was added to a solution of carbon tetrabromide (8.46g, 25.5 mmol) in CH_2Cl_2 (dry, 200 mL) resulting in an orange mixture. Then a solution of 1,5-bis(trimethylsilyl)-1,4 -pentadiyn-3-one (**2**) (3.77g, 17 mmol) in CH_2Cl_2 (40 mL) was added dropwise to this mixture over the course of 30 minutes, resulting in a further color change to deep red. The reaction was monitored by TLC and after stirring for 1 hour at room temperature it was found to be give complete conversion of the starting material. The mixture was concentrated under reduced pressure to approximately 50 mL. After the addition of *n*-hexane (~100 mL), the reaction mixture was filtered through a short plug of silica. The filtrate was dried with Na_2SO_4, filtered and concentrated to give a bright yellow oil. This oil was further purified by flash chromatography (*n*-hexane, silica) giving 3-(dibromomethylidene)-1,5-bis(trimethylsilyl)penta-1,4-diyne (**1**) as a colorless oil in 92% yield (5.94 g). ^{1}H NMR δ [ppm]: 0.23 (s, 18 H). ^{13}C NMR δ [ppm]: 114.73, 110.96, 103.1, 100.5, -0.0.

Synthesis of 3-(dibromomethylene)penta-1,4-diyne (2).[1]

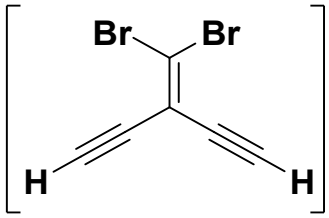

K_2CO_3 (0.15 g) was added to a solution of (3-(dibromomethylene)penta-1,4-diyne-1,5-diyl)bis(trimethylsilane) (0.335 g, 0.88 mmol) in MeOH (35 mL). The reaction mixture was allowed to stir for 1 hour and before it was poured into DI water. The mixture was extracted with *n*-pentane and dried over Na_2SO_4. The organic phase was filtered and concentrated by evaporation at 30 ℃. 3-(Dibromomethylene)penta-1,4-diyne (**2**) was obtained as a colourless needle-like crystals in quantitative yield. The compound was used directly in the polymerization reaction without further purification.

Preparation of 2D-PCM. 3-(Dibromomethylene)penta-1,4-diyne (3.95 g, 16.9 mmol) was dissolved in *N*,*N*-dimethylformamide (anhydrous, 100 mL). The resulting solution was added

to the mixture of tetrakis(triphenylphosphine)palladium(0) (980 mg, 0.845 mmol), copper iodide (322 mg, 1.7 mmol), *N*,*N*-dimethylformamide (anhydrous, 40 mL) and triethylamine (60 mL). The reaction mixture was heated to 150 °C and stirred for 72 hours under an argon atmosphere. The resulting black insoluble product was filtered off and washed four times with 150 mL DI water, ethanol, acetone and chloroform, respectively. Further purification of the product was carried out by successive Soxhlet extractions with tetrahydrofuran, methanol, and chloroform. The product was dried in vacuum for 24 hours at 120 °C to afford black powder in 90% yield (1.1 g).

NMR spectra

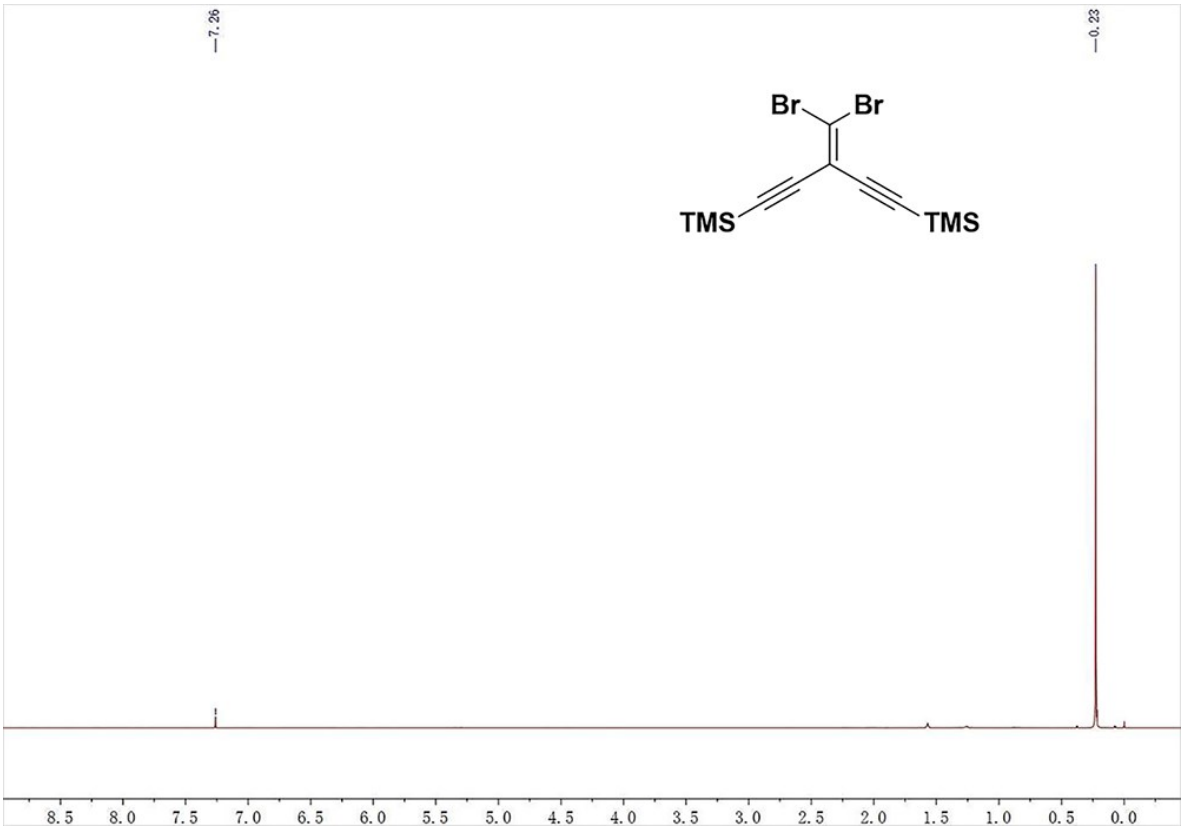

Fig. S1 ^{1}H NMR of compound **3** (400 MHz, $CDCl_3$).

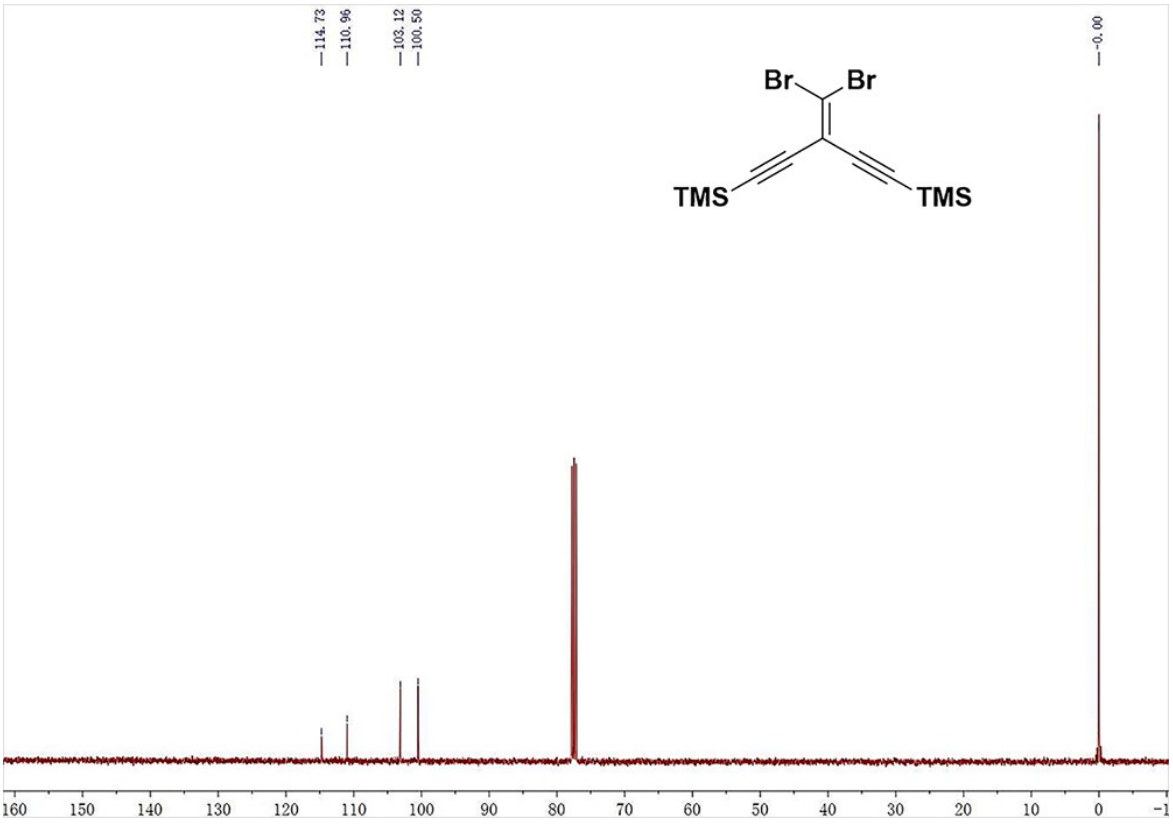

Fig. S2 ^{13}C NMR of compound **3** (100 MHz, $CDCl_3$).

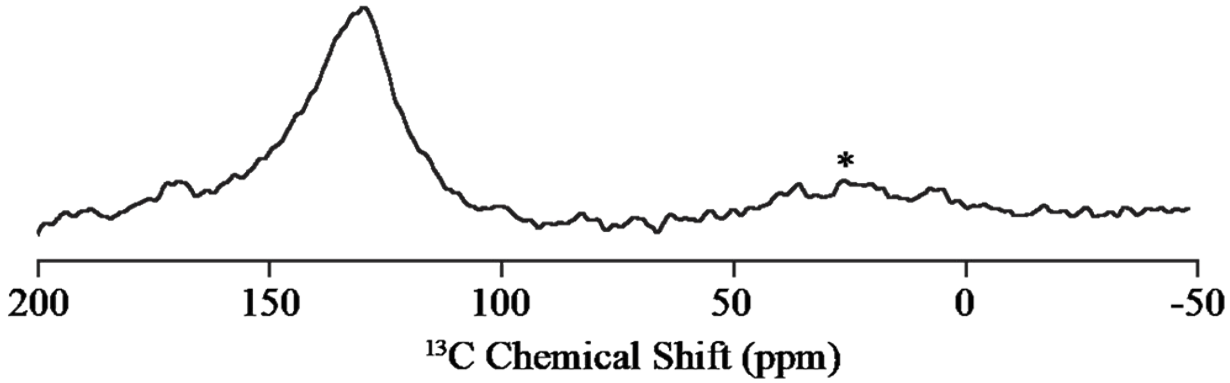

Fig. S3 Directly excited ^{13}C MAS NMR spectrum of 2D-PCM obtained after a long recycle delay of 0.5 h. The asterisk (*) denotes a spinning sideband from the sp^2-hybridized carbons at 30 ppm.

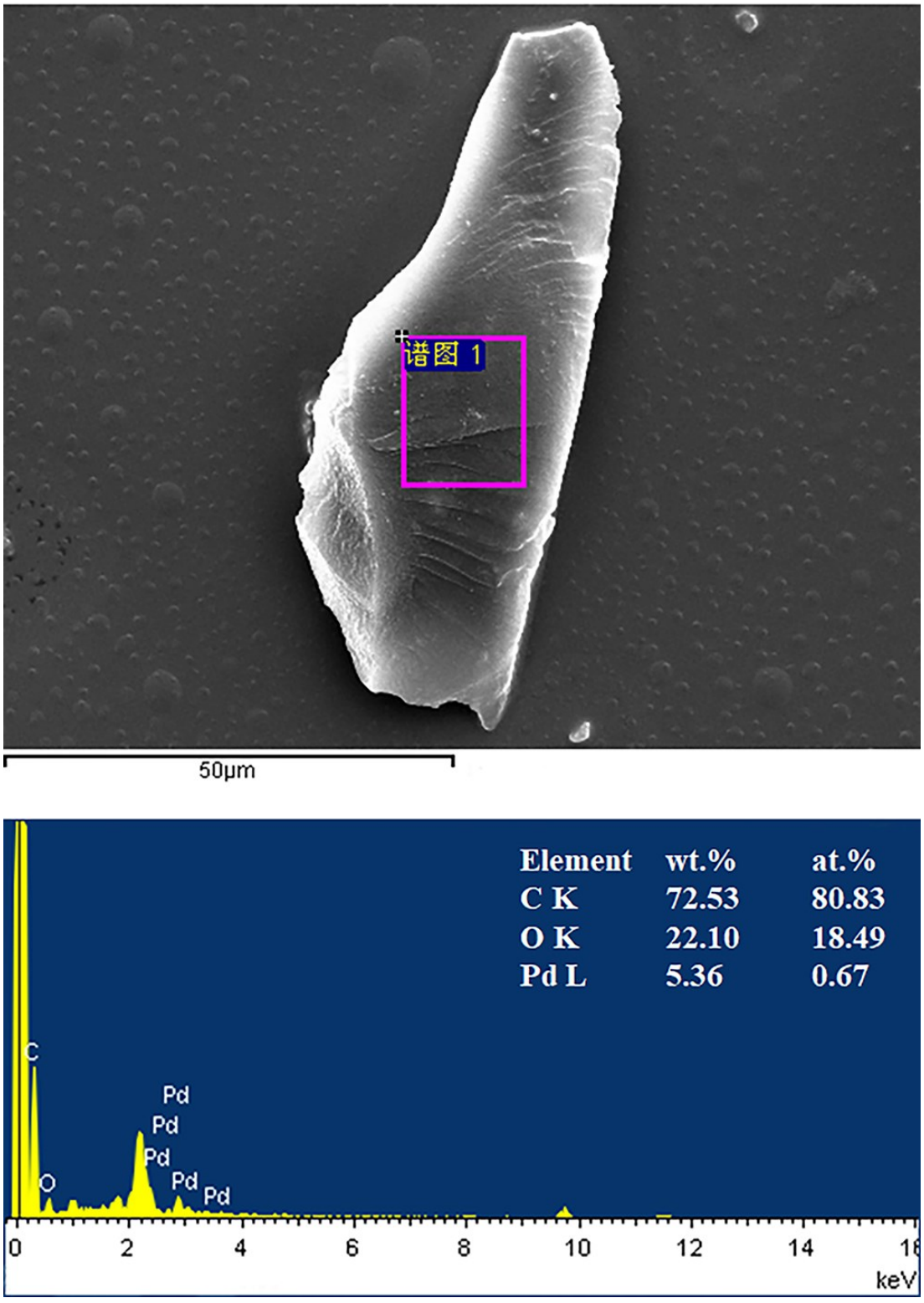

Fig. S4 Energy dispersive X-ray spectrum. The material is mainly composed of elemental carbon. The existence of oxygen is possibly due to absorbed atmospheric oxygen. Residual palladium originates from the polymerization reaction where $[Pd(PPh_3)_4]$ was used as the catalyst.

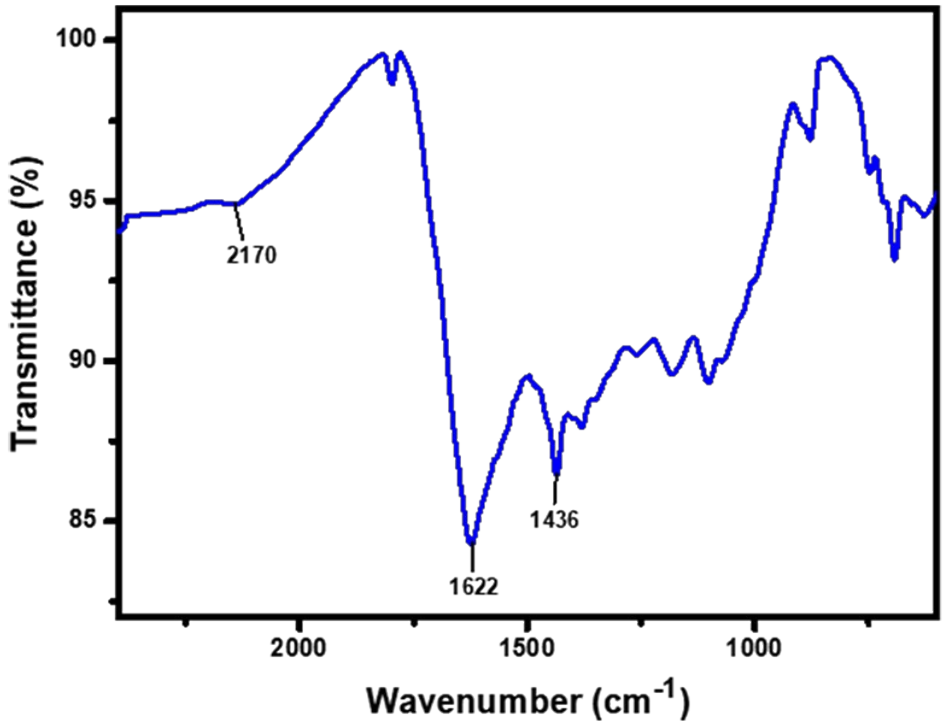

Fig. S5 FT-IR spectrum of 2D-PCM. The absorption bands located at 1436 cm^{-1}, 1622 cm^{-1} are assigned to skeletal vibrations of the aromatic rings and stretching vibrations of C=C bonds. The weak absorption band located at 2170 cm^{-1} is assigned to C≡C bond stretching vibrations, most likely terminal alkyne end groups.

Functional group experiments

The addition of bromine can be used to test for the presence of unsaturation (double and triple bonds). A sample of 2D-PCM (20 mg) was dispersed by ultrasonication in dichloromethane and a small amount of bromine were added to this sample (0.2 mmol mL^{-1}). No decolourisation of the solution was observed upon ultrasonication/shaking of the suspension, nor after leaving standing overnight.

Post-synthetic modification of 2D-PCM was also attempted. Organic dyes can be added to insoluble materials, such as graphene oxide,[26] or graphenes[27] *via* copper catalyzed click chemistry. In this case, the modification was performed with $CuSO_4$, sodium ascorbate and 3-azido-7-hydroxycoumarin (**Fig. S7**) in *N*, *N*-dimethylformamide/water at 50 °C for 2 days, before centrifugation of the suspension and washing with DMF (2 × 50 mL), water (2 × 50 mL) and methanol (2 × 50 mL). Commercial graphene monolayer (Ossila, UK) was used as a control. After workup the samples were dispersed in water and photoluminescence spectra were recorded. 3-Azido-7-hydroxycoumarin has a strong fluorescence emission around 400–450 nm in methanol solution. No emission was observed at this wavelength (**Fig. S7**) nor at around 477 nm (the manufacturer reports the shift in conjugation with DNA) after the click reaction was performed with 2D-PCM. The reaction mixture shows the characteristic emission of 3-azido-7-hydroxycoumarin, which is then lost in the work-up process indicating that it is unreacted (**Fig. S9**). A similar result was obtained for the graphene control sample.

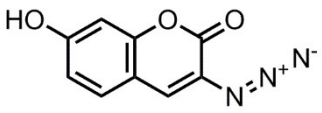

Fig. S6 Structure of 3-azido-7-hydroxycoumarin.

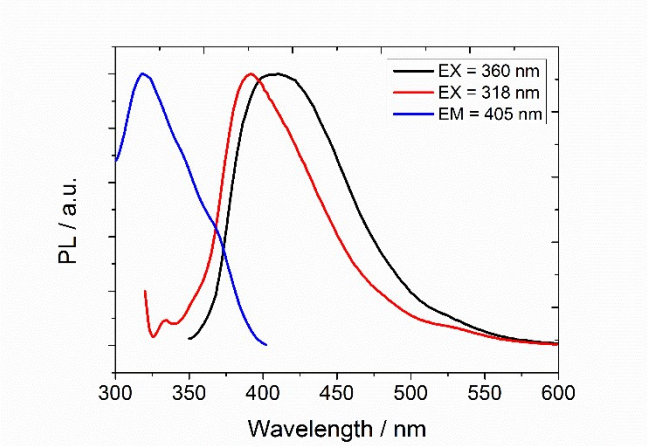

Fig. S7 Photoluminescence spectra of 3-azido-7-hydroxycoumarin in methanol solution.

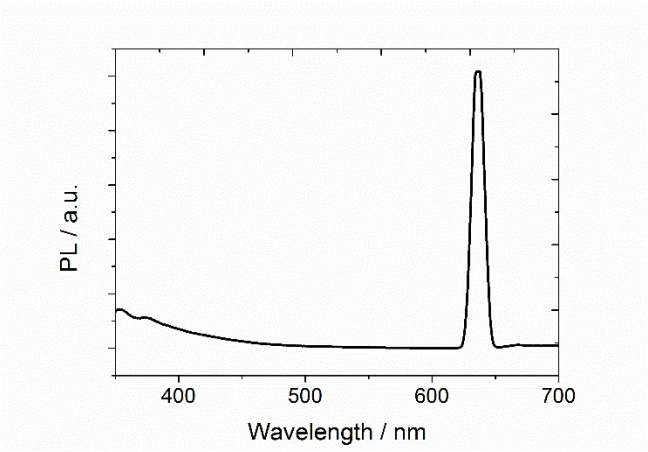

Fig. S8 Photoluminescence spectrum of 2D-PCM after attempted modification with 3-azido-7-hydroxycoumarin.

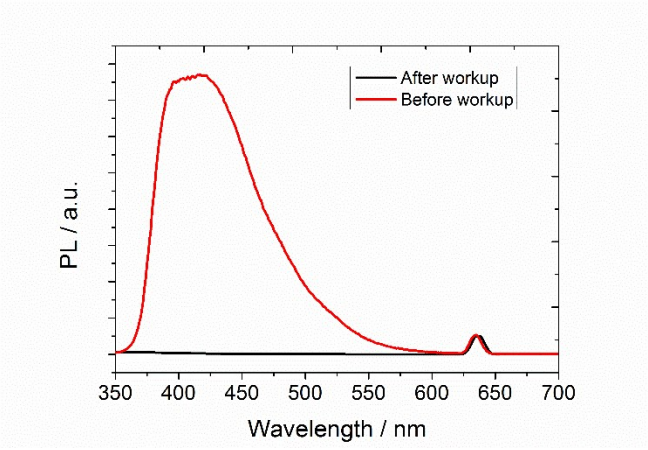

Fig. S9 PL Spectra of 2D-PCM sample in the reaction mixture before and after work-up.

Finally, 1% $KMnO_4$ (aq.) was added to a suspension of 2D-PCM in acetone, to determine if there was any unsaturation in the structure (**Fig. S10**). The addition was analysed by UV/vis spectroscopy (**Fig. S11**). Small quantities of $KMnO_4$ resulted in a change in the absorption. At these very low concentrations, this could be attributed to absorption of $KMnO_4$ at the surface of 2D-PCM rather than a chemical reaction.

Fig. S10 Photograph of 5 mg 2D-PCM sample suspended in acetone with 1% $KMnO_4$ (aq.) added (left) and the 1% $KMnO_4$ solution as made (right).

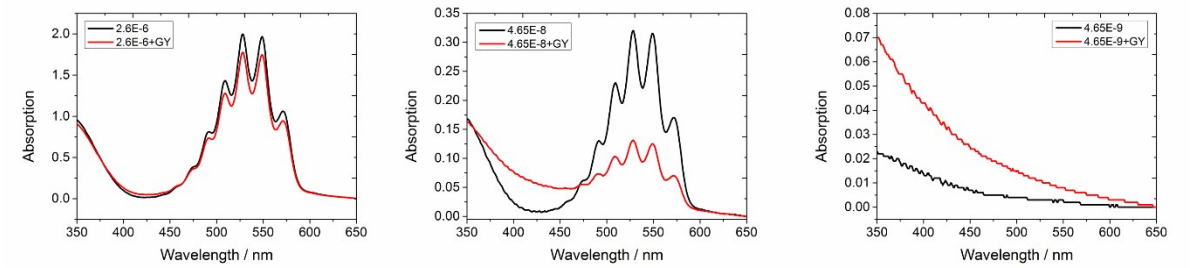

Fig. S11 UV-Vis spectra of $KMnO_4$ acetone solutions with 5 mg of 2D-PCM (see legend for concentrations given in mol L^{-1}).

Overall, no significant amount of sp-hybridised carbons was observed in 2D-PCM, in keeping with the solid state NMR data.

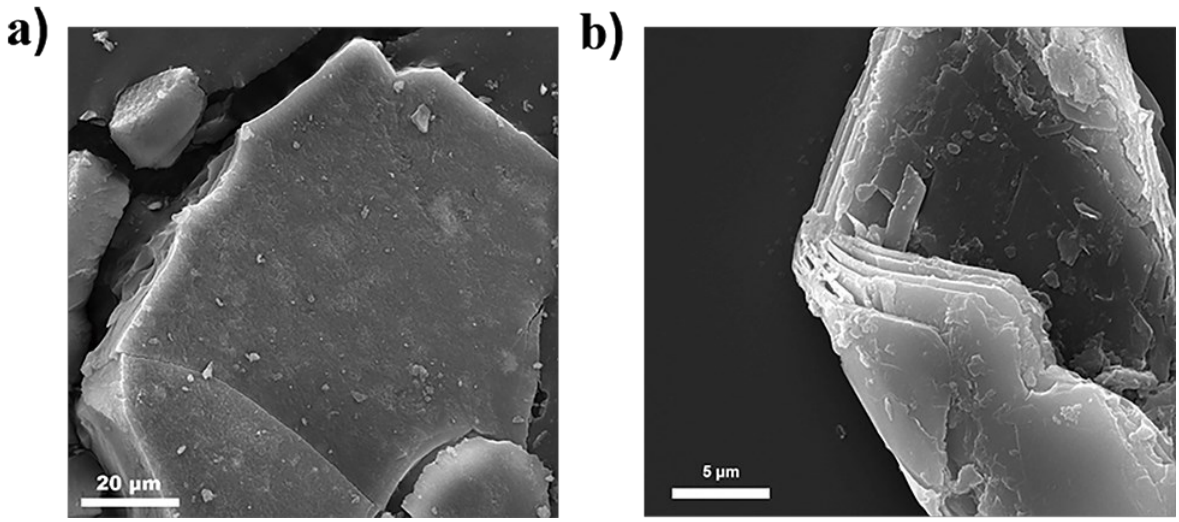

Fig. S12 a-b) Scanning electron microscope of 2D-PCM at different magnifications.

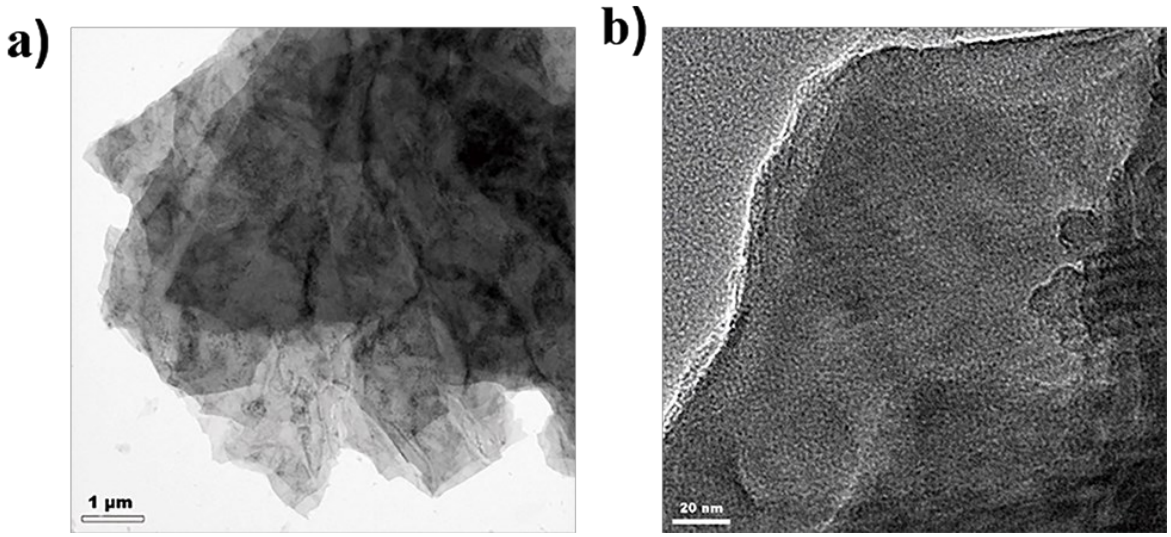

Fig. S13 a-b) Transmission electron microscope images of 2D-PCM at different magnifications.

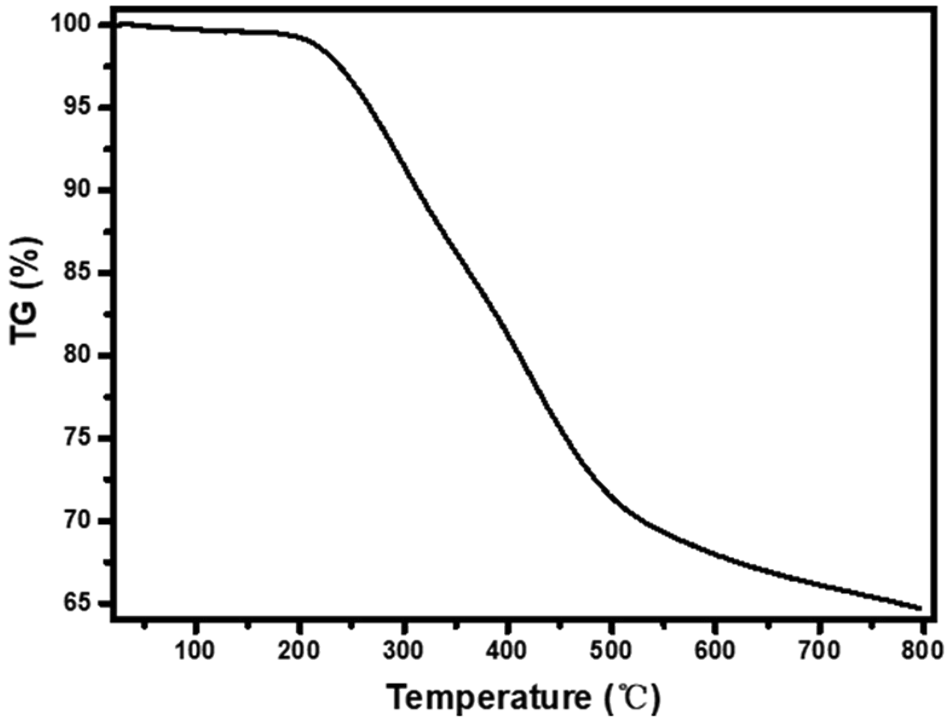

Fig. S14 Thermogravimetric analysis curve of 2D-PCM.

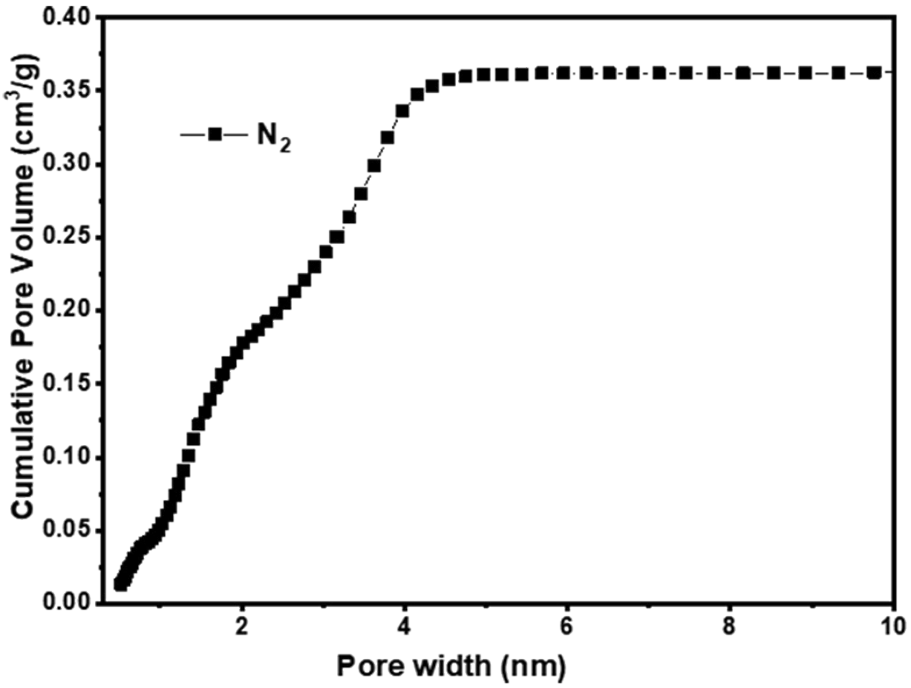

Fig. S15 Cumulative pore volumes of 2D-PCM (N_2 sorption measurement was performed on a BELSORB Max at 77 K).

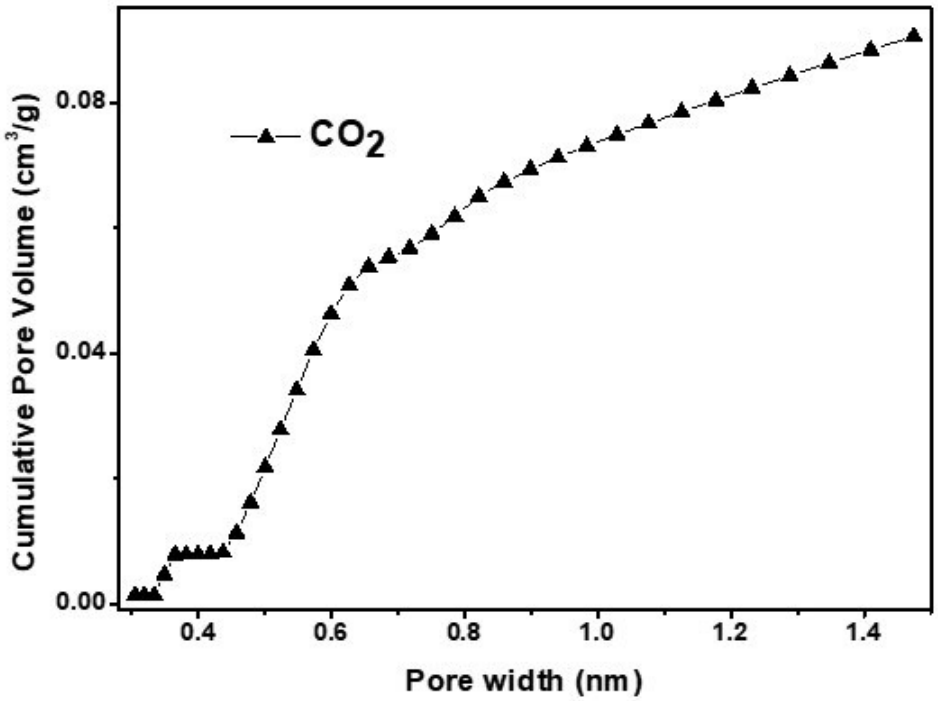

Fig. S16 Cumulative pore volumes of 2D-PCM (CO_2 sorption measurement was performed on a BELSORB Max at 273 K).

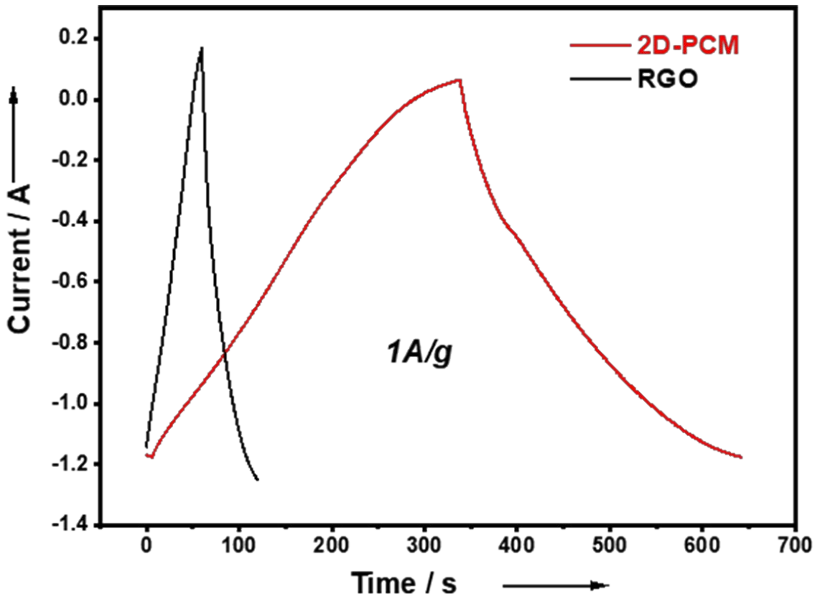

Fig. S17 Galvyanostatic charge-discharge curves of 2D-PCM and graphene at a current density of 1 A g^{-1}. The specific capacitance of 2D-PCM calculated from the slope of discharge curve at a current density of 1 A g^{-1} as is estimated to be 255 F g^{-1}. This is 6 times higher than the specific capacitance of RGO (42 F g^{-1}).

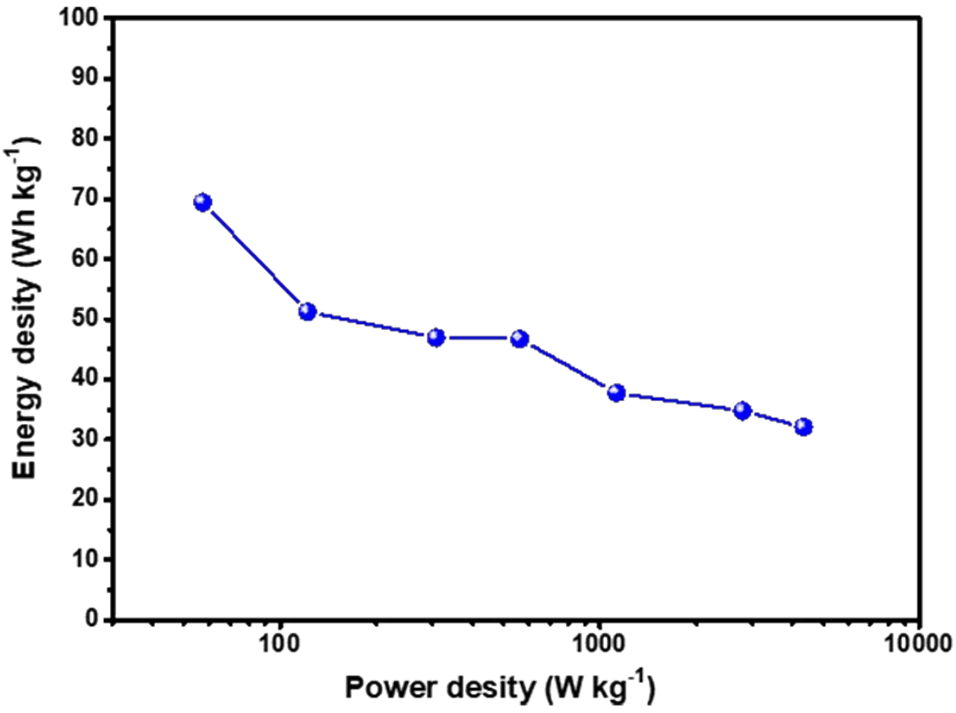

Fig. S18 Ragone plots for 2D-PCM.

Table S1. Comparison of gravimetric capacitances of various carbon-based electrode materials reported in the literature.

Material	Gravimetric capacitance	Electrolyte	Reference
Reduced graphene oxide	42.3 (1 A g^{-1})	6 M KOH	This work
	41.5 (0.1 A g^{-1})	6 M KOH	**4**
a-MEGO	165 (1.4 A g^{-1})	$BMIMBF_4$/AN	**5**
Graphene/CNT	110 (1 A g^{-1})	1 M $TEABF_4$/ PC	**6**
RGO/AC	117 (1 A g^{-1})	1 M $TEABF_4$	**7**
Activated carbon xerogel	251 (0.125 A g^{-1})	1 M H_2SO_4	**8**
Porous carbon	262 (2 mV s^{-1})	1 M H_2SO_4	**9**
	115 (0.05 A g^{-1})	6 M KOH	**10**
2D porous carbon nanosheets	244–304 (0.1 A g^{-1})	6 M KOH	**11**
3D porous carbon	176 (10 mV s^{-1})	1 M H_2SO_4	**12**
S-Porous carbon/graphene	109 (0.05 A g^{-1})	6 M KOH	**13**
Nitrogen-enriched nonporous carbon	198 (0.05 A g^{-1})	1 M H_2SO_4	**14**
Nitrogen-doped holey graphitic carbon	206 (0.1 A g^{-1})	6 M KOH	**15**
Boron-doped graphene	155 (1 A g^{-1})	6 M KOH	**16**
3D nitrogen and boron co-doped graphene	239 (1 A g^{-1})	1 M H_2SO_4	**17**
B-/ N-porous carbon	247 (0.5 A g^{-1})	6 M KOH	**18**
MOF-derived nanoporous carbon	251 (5 mV s^{-1})	1 M H_2SO_4	**19**
2D conductive MOF	396 (0.2 A g^{-1})	/	**20**
2D COF	256, 538 (0.2 A g^{-1})	1 M H_2SO_4	**21**
CTF-0	151 (0.1 A g^{-1})	$EMIMBF_4$	**22**
CTF-1	220–298 (0.2 A g^{-1})	1 M H_2SO_4	**23**
Graphdiyne	178 (0.5 A g^{-1})	1 M $LiPF_6$/EC/DMC	**24**
	71 (3.5 A g^{-1})	1 M Na_2SO_4	**25**

2D-PCM	**377.8 (0.1 A g^{-1})**	**6 M KOH**	**This work**
	254.5 (1 A g^{-1})		
	174.5 (10 A g^{-1})		

References

1. N.P. Bowling and R. J. McMahon, *J. Org. Chem.,* 2006, **71**, 5841-5847.
2. B. M. Fung, A. K. Khitrin and K. Ermolaev, *J. Magn. Reson.,* 2000, **142**, 97-101.
3. C. R. Morcombe and K. W. Zilm, *J. Magn. Reson.,* 2003, **162**, 479-486.
4. Z. Lei, N. Christov, X. S. Zhao, *Energy Environ. Sci.,* 2011, **4**, 1866-1873.
5. Y. Zhu, S. Murali1, M. D. Stoller, K. J. Ganesh, W. Cai, P. J. Ferreira1, A. Pirkle, R. M. Wallace, K. A. Cychosz, M. Thommes, D. Su, E. A. Stach and R. S. Ruoff, *Science,* 2011, **332**, 1537-1541.
6. N. Jung, S. Kwon, D. Lee, D. M. Yoon, Y. M. Park, A. Benayad, J. Y. Choi and J. S. Park, *Adv. Mater.,* 2013, **25**, 6854-6858.
7. Q. Zhou, J. Gao, C. Li, J. Chen and G. Shi, *J. Mater. Chem. A,* 2013, **1**, 9196-9201.
8. Z. Z. Benabithe, F. C. Marín, J. de Vicente and C, M. Castilla, *Langmuir,* 2013, **29**, 6166-6173.
9. E. R. Piñero, F. Leroux and F. Béguin, *Adv. Mater.,* 2006, **18**, 1877-1882.
10. B. Xu, F. Wu, S. Chen, Z. Zhou, G. Cao and Y. Yang, *Electrochim. Acta,* 2009, **54**, 2185-2189.
11. X. Zhuang, F. Zhang, D. Wu, Ni. Forler, H. Liang, M. Wagne, D. Gehrig, M. R. Hansen, F. Laquai and X. L. Feng, *Angew. Chem. Int. Ed.,* 2013, **52**, 9668-9672.
12. Z. Wu, Y. Sun, Y. Tan, S. Yang, X. Feng and K. Müllen, *J. Am. Chem. Soc.,* 2012, **134**, 19532-19535.
13. M. Seredych and T.J. Bandosz, *J. Mater. Chem. A,* 2013, **1**, 11717-11727.
14. D. H. Jurcakova, M. Kodama, S. Shiraishi, H. Hatori, Z. Zhu and G. Lu, *Adv. Funct. Mater.,* 2009, **19**, 1800-1809.
15. Z. Xiang, D. Cao, L. Huang, J. Shui, M. Wang and L. Dai, *Adv. Mater.,* 2014, **26**, 3315-3320.
16. J. Han, L. Zhang, S. Lee, J. Oh, K. S. Lee, J. R. Potts, J. Ji, X. Zhao, R. S. Ruoff and S. Park, *ACS Nano,* 2012, **7**, 19-26.

17. Z. Wu, A. Winter, L. Chen, Y. Sun, A. Turchanin, X. Feng and K. Müllen, *Adv. Mater.,* 2012, **24**, 5130-5135.
18. D. Guo, J. Mi, G. Hao, W. Dong, G. Xiong, W. Li and A. Lu, *Energy Environ. Sci.,* 2013, **6**, 652-659.
19. R. R. Salunkhe, Y. Kamachi, N. L. Torad, S. M. Hwang, Z. Sun, S. Dou, J. H. Kimc and Y. Yamauchi, *J. Mater. Chem. A,* 2014, **2**, 19848-19854.
20. J. Liu, X. Song, Y. Zhou, Z. Xie, Y. Li, Y. Liu, J. Sun, Y. Ma, O. Terasaki and L. Chen, *Angew. Chem.-Int. Edit.*, 2020, **59**, 1081-1086.
21. M. Li, J. Liu, Y. Li, G. Xing, X. Yu, C. Peng and L. Chen, *CCS Chem.*, 2020, **2**, 696-706.
22. L. Hao, J. Ning, B. Luo, B. Wang, Y. Zhang, Z. Tang, J. Yang, A. Thomas and L. Zhi, *J. Am. Chem. Soc.,* 2015, **137**, 219-225.
23. L. Hao, B. Luo, X. Li, M. Jin, Y. Fang, Z. Tang, Y. Jia, M. Liang, A. Thomas, J. Yang and L. Zhi, *Energy Environ. Sci.,* 2012, **5**, 9747-9751.
24. H.Du, H.Yang, C. Huang, J. He, H. Liu and Y. Li, *Nano Energy,* 2016, **22**, 615-622.
25. K.Krishnamoorthy, S. Thangavelab, J. C. Veetil, N. Raju, G. Venugopal and S. J. Kim, *Int. J. Hydrogen Energy,* 2016, **41**, 1672-1678.
26. R. Kurapati, F. Bonachera, J. Russier, A. R. Sureshbabu, C. M. Moyon, K. Kostarelos and A. Bianco, *2D Materials.,* 2017, **5**, 015020.
27. Y. Pan, H. Bao, N. G. Sahoo, T. Wu and L. Li, *Adv. Funct. Mater.,* 2011, **21**, 2754.1